Preprints of the 19th World Congress
The International Federation of Automatic Control
Cape Town, South Africa. August 24-29, 2014

Adaptive filtering approach to dynamic weighing: a checkweigher case study

Michał Meller * **Maciej Niedźwiecki** * **Przemysław Pietrzak** **

* *Faculty of Electronics, Telecommunications and Informatics, Department of Automatic Control, Gdańsk University of Technology, Narutowicza 11/12, 80-233 Gdańsk , Poland*
** *Department of Control and Measurement, West Pomeranian University of Technology, Sikorskiego 37, 70-313 Szczecin, Poland*
e-mail: michal.meller@eti.pg.gda.pl, maciekn@eti.pg.gda.pl, pietrzak@zut.edu.pl

Abstract: Dynamic weighing, i.e., weighing of objects in motion, without stopping them on the weighing platform, allows one to increase the rate of operation of automatic weighing systems used in industrial production processes without compromising their accuracy. The paper extends and compares two approaches to dynamic weighing, based on system identification and variable-bandwidth filtering, respectively. Experiments, carried on a conveyor belt type checkweigher, show that when appropriately tuned, both approaches yield satisfactory results that meet stringent metrological accuracy specifications.

Keywords: Dynamic weighing, system identification, variable-bandwidth filtering.

1. INTRODUCTION

In static weighing systems the weighed object is placed on the scale's platform and remains there, in a fixed position, until the weight measurements settle down, reaching their steady state value. Even though such a scenario guarantees high precision and repeatability of measurements, it also has some obvious drawbacks, such as the limited weighing capacity due to the long operating cycle. In an alternative solution, called dynamic weighing, the static weight of an object, which moves over the weighing platform or is placed there for a very short time, is assessed based on the scale's transient response.

Dynamic weighing is a convenient solution in road and rail transportation monitoring systems, as it allows one to check the weight of a vehicle (e.g. a truck or a freight train) without stopping it on the weighing platform.

Another practically important application, which will be of our main interest here, is checking the weight of pre-assembled products prior to packing them. Automatic catch weighing instruments (catchweighers) used for this purpose are usually a part of production lines and are integrated into a load transport system. An example of a conveyor-based catchweigher is schematically depicted in Fig. 1, and its basic operating cycle – in Fig. 2. The weighing section of the conveyer is mounted on a strain gauge load cell; additionally the system is equipped with two photocells located between the in-feed and weighing conveyor, and between the weighing and out-feed conveyor, respectively. Signals obtained from both photocells allow one to precisely localize transient periods during which the weighted objects slide on and off the weighing platform. A typical signal collected during a single measurement cycle is shown in Fig. 3.

The main challenge one faces when designing a dynamic weighing system is providing high measurement accuracy, especially at high conveyor belt speeds. Since at the end of each weighing cycle the weighing platform still oscillates, the mass of the weighed object can't be measured in a direct way - the signal obtained from the strain gauge must be processed in a special way in order to "extract" this information from the transient response of the system. Basically, two different approaches to dynamic weighing were described in the literature.

The approach, based on system identification, was first proposed in (Shu, 1993) (for catchweighers) and later rediscovered, in a different context, in (Niedźwiecki & Wasilewski, 1996) and (Niedźwiecki & Wasilewski, 1997) (for dynamic weighing of vehicles). In this approach, the measured signal is modeled as a response of a second-order dynamic system with unknown parameters, to a pulse-like excitation. During each operating cycle, parameters of the best-fitting model of the system are estimated based on the available measurements. Once the model is identified, its steady-state response to a step-like excitation (i.e., the static weight of the deployed object) can be easily calculated.

Unlike the first approach, the second approach to dynamic weighing is not based on any physically motivated model of the catchweighing instrument. Instead of this, a special linear lowpass filter is designed, with time-varying coefficients selected so as to quickly attenuate the narrowband disturbance component of the measured signal (Piskorowski, 2008), (Piskorowski & de Anda, 2009), (Pietrzak, 2010). The output of such a variable-bandwidth filter converges much faster to the steady state value of the system response than the analogous output of a conventional time-invariant (i.e., fixed-bandwidth) filter.

2. EXPERIMENTAL DATA

To carry out experiments, an instrument made up of three conveyor belts, depicted in Fig. 1, was used. The length of the weighing section was equal to $L = 350$ mm.

Copyright © 2014 IFAC

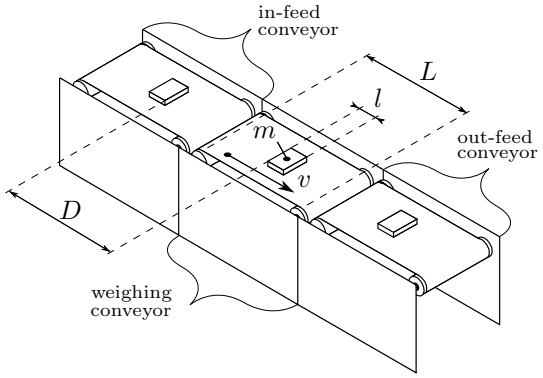

Fig. 1. A conveyor belt type checkweigher.

Two sets of measurements were taken – one for the purpose of training (used only in variable-bandwidth filter experiments), and one for performance evaluation purposes. To obtain the training set, 4 different objects (metal bars of length $l = 142$ mm), with masses of $m_1 = 200$ g, $m_2 = 300$ g, $m_3 = 500$ g and $m_4 = 700$ g, respectively, were weighed for 5 conveyor belt speeds ranging from $v = 0.5$ m/s to $v = 1.3$ m/s. For each test load and each conveyor belt speed, weighing was repeated 20 times. The evaluation set was obtained by means of repeating 20 times, for each conveyor belt speed, the sequence of 4 weighings performed for test loads m_4, m_1, m_3 and m_2 (in the indicated order). In all cases mentioned above the signals obtained from the load cell and two photocells were sampled at the rate of 1.6 kHz and stored on the computer hard disk. In total, the results of 800 weighings were cataloged – 400 for training and 400 for performance evaluation purposes.
The desired metrological catchweigher parameters, corresponding to class XIII accuracy, are summarized in Tab. 1 - see (International accuracy recommentation, 2006). Note that in all cases the admissible absolute mean errors $|\mu|_{\max}$ and the corresponding standard error deviations $\sigma_{\max}$ do not exceed the level of 0.25% of the true weight.

Table 1. Desired metrological parameters for the accuracy class XIII checkweighers.

test load [g]	$\lvert\mu\rvert_{\max}$ [g]	$\sigma_{\max}$ [g]
200	0.25	0.48
300	0.5	0.48
500	0.5	0.8
700	0.5	0.8

3. SYSTEM IDENTIFICATION BASED APPROACH

3.1 Model-based weight estimation

Taking the "black box" approach, the dynamics of a weighing mechanical structure can be approximated by the following linear model

$$y(t) = H(q^{-1})u(t) \tag{1}$$

$$H(q^{-1}) = \frac{b_1 q^{-1} + \ldots + b_p q^{-p}}{1 + a_1 q^{-1} + \ldots + a_r q^{-r}}, \quad p \le r$$

where $t = \ldots, -1, 0, 1, \ldots$ denotes normalized (dimensionless) discrete time, $u(t)$ denotes the unknown time-varying load signal, $y(t)$ denotes the signal obtained from the load cell, and q^{-1} denotes the backward shift operator: $q^{-1}x(t) = x(t-1)$.

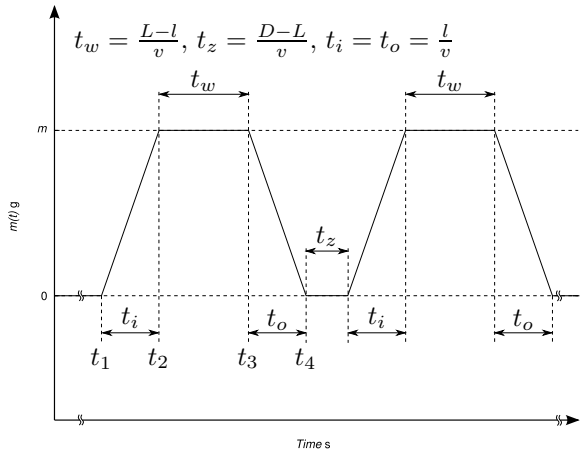

Fig. 2. Weighing cycle of a conveyor belt type checkweigher.

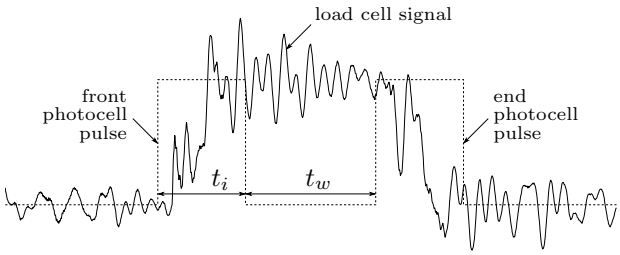

Fig. 3. Typical responses of the load cell and front/end photocells observed during one weighing cycle.

Suppose that the system governed by (1) is excited by the step signal $u(t) = u_0 1(t)$, where $1(t)$ denotes the unit step function. Then the steady state system response will take the form

$$y_\infty = \lim_{t\to\infty} y(t) = H(1)u_0 \tag{2}$$

(provided that the limit exists, i.e., the filter $H(q^{-1})$ is stable). Note that in the case of checkweigher this steady state value corresponds to the static weight $w = mg$ of the weighed object.
After incorporating the noise component into the deterministic system description (1), one arrives at the following ARX(r,p) (autoregressive with exogenous input) model

$$y(t) + \sum_{i=1}^{r} a_i y(t-i) = \sum_{i=1}^{p} b_i u(t-i) + n(t) \tag{3}$$

where $n(t)$ denotes white input noise. In this stochastic context the quantity y_∞, given by (2), can be interpreted as the steady state mean value of the output signal: $y_\infty = \lim_{t\to\infty} \mathrm{E}[y(t)]$.
Note that the model (3) can be written down in a more compact form

$$y(t) = \boldsymbol{\varphi}^{\mathrm{T}}(t)\boldsymbol{\theta} + n(t) = \boldsymbol{\varphi}_y^{\mathrm{T}}(t)\boldsymbol{\theta}_y + \boldsymbol{\varphi}_u^{\mathrm{T}}(t)\boldsymbol{\theta}_u + n(t) \tag{4}$$

where the quantities $\boldsymbol{\theta} = [\boldsymbol{\theta}_y^{\mathrm{T}}, \boldsymbol{\theta}_u^{\mathrm{T}}]^{\mathrm{T}}$, $\boldsymbol{\theta}_y = [a_1, \ldots, a_r]^{\mathrm{T}}$ and $\boldsymbol{\theta}_u = [b_1, \ldots, b_p]^{\mathrm{T}}$ denote the vectors of model coefficients, and $\boldsymbol{\varphi}(t) = [\boldsymbol{\varphi}_y^{\mathrm{T}}(t), \boldsymbol{\varphi}_u^{\mathrm{T}}(t)]^{\mathrm{T}}$, $\boldsymbol{\varphi}_y(t) = [-y(t-1), \ldots, -y(t-r)]^{\mathrm{T}}$ and $\boldsymbol{\varphi}_u(t) = [u(t-1), \ldots, u(t-p)]^{\mathrm{T}}$ denote the corresponding regression vectors.
When model coefficients are not known, they can be replaced with the corresponding estimates. Suppose that N data pairs $\{y(1), \boldsymbol{\varphi}(1)\}, \ldots, \{y(N), \boldsymbol{\varphi}(N)\}$ are available.

Then, if the regression matrix $\mathbf{R}(N) = \sum_{t=1}^{N} \boldsymbol{\varphi}(t)\boldsymbol{\varphi}^{\mathrm{T}}(t)$ is nonsingular, i.e., invertible, the least squares (LS) estimate of $\boldsymbol{\theta}$ takes the form

$$\widehat{\boldsymbol{\theta}}(N) = \mathbf{R}^{-1}(N)\mathbf{s}(N) \tag{5}$$

where $\mathbf{s}(N) = \sum_{t=1}^{N} \boldsymbol{\varphi}(t)y(t)$. Note that the estimate $\widehat{\boldsymbol{\theta}}(N) = [\widehat{\boldsymbol{\theta}}_y^{\mathrm{T}}(N), \widehat{\boldsymbol{\theta}}_u^{\mathrm{T}}(N)]^{\mathrm{T}}$ given by (5) is a solution of the equation

$$\begin{bmatrix} \mathbf{R}_y(N) & \mathbf{R}_{yu}(N) \\ \mathbf{R}_{yu}^{\mathrm{T}}(N) & \mathbf{R}_u(N) \end{bmatrix} \begin{bmatrix} \widehat{\boldsymbol{\theta}}_y(N) \\ \widehat{\boldsymbol{\theta}}_u(N) \end{bmatrix} = \begin{bmatrix} \mathbf{s}_y(N) \\ \mathbf{s}_u(N) \end{bmatrix} \tag{6}$$

where

$$\mathbf{R}_y(N) = \sum_{t=1}^{N} \boldsymbol{\varphi}_y(t)\boldsymbol{\varphi}_y^{\mathrm{T}}(t), \quad \mathbf{R}_u(N) = \sum_{t=1}^{N} \boldsymbol{\varphi}_u(t)\boldsymbol{\varphi}_u^{\mathrm{T}}(t)$$

$$\mathbf{R}_{yu}(N) = \sum_{t=1}^{N} \boldsymbol{\varphi}_y(t)\boldsymbol{\varphi}_u^{\mathrm{T}}(t)$$

$$\mathbf{s}_y(N) = \sum_{t=1}^{N} \boldsymbol{\varphi}_y(t)y(t), \quad \mathbf{s}_u(N) = \sum_{t=1}^{N} \boldsymbol{\varphi}_u(t)y(t)$$

Replacing in (2) the true values of system coefficients with the corresponding estimates, one arrives at the following weight estimate

$$\widehat{w}(N) = \widehat{H}(1)u_0 = \frac{\sum_{i=1}^{p} \widehat{b}_i(N)}{1 + \sum_{i=1}^{r} \widehat{a}_i(N)}\, u_0 \tag{7}$$

The estimation formula (7) remains valid if the excitation (load) signal is modeled more realistically, as a finite-duration trapezoidal pulse (see Fig. 2)

$$u(t) = \begin{cases} 0 & \text{for} \quad t < t_1 \\ \dfrac{t - t_1}{t_2 - t_1}\, u_0 & \text{for} \quad t \in [t_1, t_2) \\ u_0 & \text{for} \quad t \in [t_2, t_3] \\ \dfrac{t_4 - t}{t_4 - t_3}\, u_0 & \text{for} \quad t \in (t_3, t_4] \\ 0 & \text{for} \quad t > t_4 \end{cases} \tag{8}$$

which consists of an ascending ramp, plateau, and descending ramp, respectively. In the case of conveyor belt checkweigher such a form of the hypothetical input signal seems to be physically well justified, since the weighed object gradually slides on the weighing conveyor, remains there for a certain amount of time, and then gradually slides of – the instances $t_1, \ldots, t_4$ can be easily determined by analyzing the pulse-like signals obtained from the front/end photocells (see Fig. 3).

However, the main problem applying the proposed approach is due to the fact that the height u_0 of the input pulse, which is proportional to the static weight of the object, is *not known* – actually it is a subject of our investigation. For this reason we will examine the consequences of adopting an incorrect value of u_0. Suppose that all calculations are based on the assumption that the height of the pulse is equal to $u_0' = \gamma u_0$, where $\gamma > 0$, $\gamma \neq 1$, i.e. that the input signal is given by $u'(t) = \gamma u(t)$. Note that the regression vector has in this case the form $\boldsymbol{\varphi}'(t) = [\boldsymbol{\varphi}_y^{\mathrm{T}}(t), \gamma\boldsymbol{\varphi}_u^{\mathrm{T}}(t)]^{\mathrm{T}}$, and the LS estimate of $\boldsymbol{\theta}$ becomes

$$\widehat{\boldsymbol{\theta}}'(N) = [\mathbf{R}'(N)]^{-1}\mathbf{s}'(N) \tag{9}$$

where $\mathbf{R}'(N)$ and $\mathbf{s}'(N)$ are made up of the following blocks: $\mathbf{R}_y'(N) = \mathbf{R}_y(N)$, $\mathbf{R}_{yu}'(N) = \gamma\mathbf{R}_{yu}(N)$, $\mathbf{R}_u'(N) = \gamma^2\mathbf{R}_u(N)$, $\mathbf{s}_y'(N) = \mathbf{s}_y(N)$, and $\mathbf{s}_u'(N) = \mathbf{s}_u(N)$. Note also, that the following identity holds true

$$\begin{aligned} \mathbf{R}'(N) \begin{bmatrix} \widehat{\boldsymbol{\theta}}_y(N) \\ \dfrac{1}{\gamma}\, \widehat{\boldsymbol{\theta}}_u(N) \end{bmatrix} &= \begin{bmatrix} \mathbf{R}_y(N) & \gamma\mathbf{R}_{yu}(N) \\ \gamma\mathbf{R}_{yu}^{\mathrm{T}}(N) & \gamma^2\mathbf{R}_u(N) \end{bmatrix} \begin{bmatrix} \widehat{\boldsymbol{\theta}}_y(N) \\ \dfrac{1}{\gamma}\, \widehat{\boldsymbol{\theta}}_u(N) \end{bmatrix} \\ &= \begin{bmatrix} \mathbf{s}_y(N) \\ \gamma\mathbf{s}_u(N) \end{bmatrix} = \mathbf{s}'(N) \end{aligned} \tag{10}$$

leading to the conclusion that

$$\widehat{\boldsymbol{\theta}}_y'(N) = \widehat{\boldsymbol{\theta}}_y(N), \quad \widehat{\boldsymbol{\theta}}_u'(N) = \frac{1}{\gamma}\, \widehat{\boldsymbol{\theta}}_u(N)$$

Substituting these estimates into the weight evaluation formula, one arrives at

$$\widehat{w}'(N) = \widehat{H}'(1)u_0' = \frac{\frac{1}{\gamma} \sum_{i=1}^{p} \widehat{b}_i(N)}{1 + \sum_{i=1}^{r} \widehat{a}_i(N)}\, \gamma u_0 = \widehat{w}(N) \tag{11}$$

which means that in spite of the errorneous assumption about the height of the input pulse, one obtains the correct estimate of w (as if the adopted value of u_0 was equal to the true one). Since the weight estimate depends on the product $[\sum_{i=1}^{p} \widehat{b}_i(N)]u_0$, rather than independently on the quantities $\sum_{i=1}^{p} \widehat{b}_i(N)$ and u_0, this self-correcting property of the proposed estimation scheme is hardly surprising.

According to (11), the weight estimate does not depend on the adopted value of u_0. This means that for the purpose of evaluation of $\widehat{w}$, one can choose *any* value of $u_0 > 0$, e.g. $u_0 = 1$.

3.2 Classical approach

The estimation schemes proposed so far were based on the second-order model ($r = 2$) identified in the constant excitation phase of system operation

$$u(t) \equiv u_0, \quad \forall t \in [t_2, t_3] \tag{12}$$

The choice of the second-order model was physically motivated. Such a model corresponds to the single degree of freedom mass-spring-damper representation of the weighing mechanical structure (Shu, 1993), (Niedźwiecki & Wasilewski, 1996).

Note that under constant excitation (12), the input/output relationship (3) can be equivalently expressed in the form

$$y(t) + \sum_{i=1}^{r} a_i y(t-i) = \beta u(t-1) + n(t) \tag{13}$$

where $\beta = \sum_{i=1}^{p} b_i$. For this reason, for a constant input signal, the identified transfer function must have the form

$$H(q^{-1}) = \frac{\beta q^{-1}}{1 + a_1 q^{-1} + \ldots + a_r q^{-r}} \tag{14}$$

Any attempt to estimate two or more input (b-type) coefficients will fail due to the lack of sufficient persistence of excitation (Söderström & Stoica, 1988) (for a constant input signal and $p > 1$ the components of the input regression vector $\boldsymbol{\varphi}_u(t)$ are linearly dependent, causing singularity of the regression matrix).

Experimental results obtained for the ARX(2,1) model, shown in Tab. 2, are unsatisfactory – the accuracy requirements are not met even for the lowest conveyor belt speeds. In order to improve estimation results, three extensions of the basic scheme were considered: incorporation of higher-order ARX models, data prefiltering, and incorporation of an extended data set.

3.3 Higher-order models

Fig. 4 shows the energy spectrum of typical transient oscillations $y(t) - w$ observed in the interval $[t_2, t_3]$. The multi-resonant structure of this spectrum suggests that the second-order spring-mass-damper model adopted in the classical approach may be inadequate for the conveyor belt type checkweighers. Tab. 3, which shows results obtained for higher-order ARX(r,1), fully supports this claim. With growing order of autoregression r, the accuracy of weight estimates systematically improves reaching, for $r = 60$, almost satisfactory levels at slow and medium conveyor belt speeds.

3.4 Data prefiltering

The approach based on identification of high-order ARX models is rather forceful and yields results that are only partially satisfactory. For this reason the next (pretty obvious) modification that was checked out, was based on the idea of data prefiltering – rather than trying to incorporate high frequency signal components into the system model, one can remove them from the processed data *prior to* identification. The results obtained in this way are shown in Tab. 4. In this case the signal obtained from the load cell was passed through a second-order lowpass Butterworth filter with a cutoff frequency f_c=10 Hz. To avoid phase distortions and delay effects introduced by IIR (infinite impulse response) filters, the signal was processed twice: first forward in time and then in a reverse time order. Such a forward/backward processing technique allows one to realize low-complexity linear-phase filters with very good stopband attenuation properties.
According to Tab. 4, lowpass filtering of the processed signal significantly improves the accuracy of the model-based weight estimates. The results obtained for the ARX(4,1) model are entirely satisfactory for all test loads and all conveyor belt speeds. When the order of the ARX model is increased beyond 4, the results gradually deteriorate. This is not a surprising effect since high-order models tend to focus on the filter dynamics (which, in the case considered, becomes a part of the identified system) instead of the checkweigher's dynamics.

3.5 Extended data set

Since the hypothetical shape of the load signal (8) can be established by analyzing position of the front/end photocell pulses, we have checked whether estimation results could be improved by means of incorporation – at the system identification stage – the measurements collected in the entire excitation interval $[t_1, t_4]$ (trapezoidal pulse) or its fragments: $[t_1, t_3]$ (ascending step) or $[t_2, t_4]$ (descending step). Due to its "richness" such an excitation signal should allow one to obtain more accurate estimates of system coefficients, i.e., more accurate weight estimates. Note that in this case the full-order zero-pole model (1) can be identified instead of the simplified all-pole model (14). Unfortunately, all attempts to improve estimation results by working with an extended data set have failed. Tab. 5 summarizes results obtained for the ARX(4,4) model (which should be compared with the analogous results, shown in Tab. 4, for the ARX(4,1) model). In all three cases mentioned above the accuracy of weight estimates deteriorated. Most likely this is caused by the fact that the shape of the actual load signal differs from the assumed

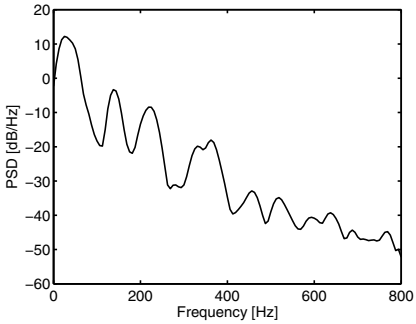

Fig. 4. Energy spectrum of transient oscillations.

(trapezoidal) one. Similar effects were observed for higher-order ARX(r, r) and ARX($r, 1$) models (both with and without data prefiltering).

Table 2. Mean weight measurement errors μ_e and their standard deviations σ_e for 5 conveyor belt speeds [m/s] and 4 test loads (m_1, m_2, m_3, m_4). All results correspond to the ARX(2,1) system representation. The values that exceed the accuracy class XIII specifications are shown in boldface.

speed		0.5	0.7	0.9	1.1	1.3
m_1	μ_e	**0.54**	**1.95**	-0.19	**0.78**	**3.56**
	σ_e	**0.48**	**1.45**	**1.61**	**1.03**	**1.75**
m_2	μ_e	**0.55**	**0.59**	**0.70**	0.19	**3.55**
	σ_e	**0.79**	**1.12**	**1.17**	**3.28**	**1.83**
m_3	μ_e	**1.22**	-0.15	**0.62**	0.06	**1.52**
	σ_e	**1.14**	**1.64**	**1.94**	**2.45**	**3.36**
m_4	μ_e	**0.73**	**2.29**	**0.55**	**-0.84**	**-4.70**
	σ_e	**1.12**	**3.05**	**1.76**	**2.28**	**3.40**

Table 3. Experimental results obtained for higher-order ARX models.

speed		0.5	0.7	0.9	1.1	1.3
ARX(20, 1)						
m_1	μ_e	0.20	**0.58**	**0.82**	-0.11	**0.66**
	σ_e	0.45	**0.62**	**0.55**	**0.89**	**0.91**
m_2	μ_e	0.41	**1.61**	0.20	**0.76**	-0.23
	σ_e	**0.49**	**0.76**	**0.80**	**0.72**	**0.98**
m_3	μ_e	**0.70**	**1.34**	-0.08	**0.75**	**1.14**
	σ_e	0.56	**1.22**	**1.11**	**1.45**	**1.89**
m_4	μ_e	**0.52**	-0.02	0.07	**0.93**	**-3.33**
	σ_e	0.63	**1.59**	**1.88**	**1.93**	**1.99**
m_4	μ_e	0.5	-0.0	0.4	**0.9**	**-3.2**
	σ_e	0.7	**1.6**	**2.0**	**2.0**	**1.8**
AR(60, 1)						
m_1	μ_e	0.07	0.23	-0.12	0.35	**-0.58**
	σ_e	0.16	0.20	0.20	**0.58**	**0.93**
m_2	μ_e	0.25	**0.60**	0.19	0.09	-0.44
	σ_e	0.18	0.38	0.39	**0.65**	**1.16**
m_3	μ_e	0.48	**0.66**	0.28	-0.19	-0.14
	σ_e	0.34	0.47	0.43	0.44	**1.22**
m_4	μ_e	0.30	0.16	-0.25	-0.03	**0.58**
	σ_e	0.37	0.48	0.63	**0.90**	0.71

Table 4. Experimental results obtained for ARX models under data prefiltering.

speed		0.5	0.7	0.9	1.1	1.3
ARX(2,1)						
m_1	μ_e	**0.73**	**0.76**	0.29	**0.54**	-0.27
	σ_e	0.32	0.38	0.27	0.20	0.31
m_2	μ_e	**0.61**	0.18	-0.26	**-0.71**	-0.13
	σ_e	**0.64**	0.46	0.37	**0.54**	**0.63**
m_3	μ_e	**1.87**	**1.54**	0.11	-0.26	-0.45
	σ_e	0.75	0.58	0.50	0.54	**1.00**
m_4	μ_e	**1.33**	**1.31**	**-1.76**	**-0.93**	**-3.19**
	σ_e	**1.42**	**1.07**	**1.21**	0.80	**1.24**
ARX(4,1)						
m_1	μ_e	-0.01	0.01	-0.12	0.25	0.10
	σ_e	0.07	0.09	0.14	0.12	0.12
m_2	μ_e	0.01	0.12	0.13	0.13	0.11
	σ_e	0.13	0.14	0.14	0.20	0.23
m_3	μ_e	0.03	0.19	-0.06	0.14	0.18
	σ_e	0.12	0.25	0.29	0.20	0.19
m_4	μ_e	-0.25	0.32	-0.10	-0.06	-0.38
	σ_e	0.19	0.38	0.24	0.38	0.32

Table 5. Experimental results obtained for the ARX(4,4) model with data prefiltering for different hypothetical excitation signals.

speed		0.5	0.7	0.9	1.1	1.3
ascending step						
m_1	μ_e	**0.4**	**2.3**	**0.5**	**1.5**	**1.1**
	σ_e	**1.0**	**1.2**	**0.7**	**1.0**	**0.9**
m_2	μ_e	-0.5	**1.8**	**0.7**	-0.2	**1.3**
	σ_e	**1.0**	**1.3**	**1.8**	**1.5**	**1.6**
m_3	μ_e	**3.3**	**5.9**	**4.7**	-0.3	**4.4**
	σ_e	**2.6**	**3.5**	**2.4**	**2.3**	**3.7**
m_4	μ_e	**12.7**	**9.7**	**9.8**	**8.8**	**12.1**
	σ_e	**4.2**	**4.0**	**8.2**	**4.5**	**8.3**
descending step						
m_1	μ_e	**2.36**	**1.23**	**-0.64**	-0.29	**-1.50**
	σ_e	**0.64**	**0.50**	0.26	0.32	0.39
m_2	μ_e	**2.04**	**1.31**	**0.88**	**-1.31**	**-1.15**
	σ_e	**0.74**	**0.59**	**0.73**	0.47	0.35
m_3	μ_e	**3.73**	**3.04**	**-1.03**	**-3.20**	**-2.67**
	σ_e	0.70	0.66	0.77	0.26	**0.82**
m_4	μ_e	**0.92**	**-2.75**	**-8.22**	**-14.05**	**-12.46**
	σ_e	**1.45**	**1.25**	**0.97**	**5.19**	**2.29**
trapezoidal pulse						
m_1	μ_e	**6.55**	**5.75**	**5.13**	**3.41**	**1.35**
	σ_e	**0.78**	**0.69**	**0.73**	**0.67**	**0.71**
m_2	μ_e	**8.25**	**6.42**	**6.31**	**5.36**	**3.49**
	σ_e	**0.90**	**0.86**	**1.13**	**1.27**	**0.61**
m_3	μ_e	**11.75**	**9.92**	**8.33**	**7.00**	**1.76**
	σ_e	**2.01**	**1.75**	**1.41**	**1.10**	**2.41**
m_4	μ_e	**13.19**	**12.61**	**5.08**	**-8.28**	**-4.44**
	σ_e	**2.93**	**1.88**	**2.93**	**5.23**	**3.39**

4. VARIABLE-BANDWIDTH FILTERING APPROACH

Another possible method, widely used in industrial applications (McGuinness et al., 2005), is to determine the static weight of the object based on the analysis of the lowpass-filtered load cell signal. As reported in (Pietrzak, 2010) good results can be achieved using a cascade connection of the first-order IIR filters of the form

$$z_i(t) + a_k z_i(t-1) = b_k[z_{i-1}(t) + z_{i-1}(t-1)] \qquad (15)$$
$$i = 1, \ldots, k, \quad t \in [t_1, t_3]$$

where k denotes the number of filters making up a cascade. The input signal entering the cascade is taken from the load cell $z_0(t) = y(t),\ t \in [t_1, t_3]$, and the weight estimate is obtained by reading out the signal observed at the output of the cascade at the instant t_3

$$\widehat{w}(N) = z_k(t_3) \qquad (16)$$

where N – the number of processed data samples – is equal to $t_3 - t_1 + 1$.

When the order-dependent filter coefficients a_k and b_k (the same for all filters) are chosen according to

$$a_k = \frac{f_c - \frac{\xi_k}{\pi\Delta}}{f_c + \frac{\xi_k}{\pi\Delta}}, \quad b_k = \frac{1+a}{2}, \quad \xi_k = \sqrt{\sqrt[k]{2} - 1} \qquad (17)$$

where Δ [s] denotes sampling period and f_c [Hz] denotes the desired cutoff frequency, equations (15) can be regarded as a discrete approximation of an analog critically dumped lowpass filter.

Further improvement can be achieved by using variable-bandwidth lowpass filters governed by

$$z_i(t) + a_k(t) z_i(t-1) = b_k(t)[z_{i-1}(t) + z_{i-1}(t-1)] \qquad (18)$$
$$i = 1, \ldots, k, \quad t \in [t_1, t_3]$$

where $a_k(t)$ and $b_k(t)$ denote time-varying coefficients obtained from (17) after replacing the time-invariant cutoff frequency f_c with its time-varying counterpart $f_c(t)$. Even though for a time-varying filter the cutoff frequency is a heuristic concept, difficult to justify in a mathematically strict manner, when used with a due caution it can be very helpful in designing filters with improved characteristics. In our current context the idea is to use a filter with a relatively large bandwidth at the initial stage of filtration (i.e., for instants t close to t_1), and to gradually reduce the bandwidth as the end of the analysis interval (t_3) is approached. Such bandwidth scheduling allows one to obtain lowpass filters with a shorter transient response, compared to response of time-invariant filters characterized by the same level of disturbance attenuation.

To achieve this goal, the time-varying "cutoff frequency" $f_c(t)$ was parameterized as follows (see Fig. 5)

$$f_c(t) = f_\infty + (f_0 - f_\infty) \exp\left\{-\alpha\left(\frac{t - t_1}{t_3 - t_1}\right)\right\} \qquad (19)$$

where $f_\infty < f_0$ and $\alpha > 0$ denotes the decay rate. According to (19), the cutoff frequency $f_c(t)$ decreases monotonically in the interval $[t_1, t_3]$ from the initial value $f_c(t_1) = f_0$ to the final value $f_c(t_3) = f_0\lambda + f_\infty(1-\lambda)$ where $\lambda = e^{-\alpha}$. Note that for sufficiently large values of α it holds that $f_c(t_3) \cong f_\infty$ (e.g. for $\alpha > 2\log 10 \cong 4.6$, one obtains $\lambda < 0.01$).

The optimal filter settings were found by searching a discretized space of filter parameters $\mathbf{w} = [f_0, f_\infty, \alpha, k]^{\mathrm{T}}$. For each conveyor belt speed $v_j, j = 1, \ldots, 5$, the best settings $\mathbf{w}_j^*$ were obtained by means of minimizing the performance measure made up of two components

$$\mathbf{w}_j^* = \arg\min_{\mathbf{w}} \{\delta_j(\mathbf{w}) + \eta_j(\mathbf{w})\} \qquad (20)$$

The first component quantifies the measurement accuracy

$$\delta_j(\mathbf{w}) = \max\left\{ \frac{|\mu_{ij}(\mathbf{w})|}{|\mu_i|_{\max}}, \frac{\sigma_{ij}(\mathbf{w})}{\sigma_{i\max}}, i = 1,\ldots,4 \right\} \quad (21)$$

where $\mu_{ij}(\mathbf{w})$ and $\sigma_{ij}(\mathbf{w})$ denote the mean error values and standard error deviations for the i-th test load ($i = 1,\ldots,4$) and the j-th conveyor belt speed ($j = 1,\ldots,5$). The quantities $|\mu_i|_{\max}$ and $\sigma_{i\max}$ denote the corresponding maximum allowable values, listed in Tab. 1.
The second component of the performance measure penalizes long transient responses and is given by

$$\eta_j(\mathbf{w}) = \max\left\{ \frac{\tau_{ij}(\mathbf{w}) - t_1}{t_3 - t_1}, i = 1,\ldots,4 \right\} \quad (22)$$

where $\tau_{ij}(\mathbf{w}) \in [t_1, t_3]$ denotes the smallest time coordinate τ, starting from which the output of the filter (18) yields weight measurements $z_k(\tau)$ that comply with the accuracy specifications summarized in Tab. 1. Note that when $\tau_{ij}(\mathbf{w}) < t_3$, then not only the last sample $z_k(t_3)$, but also a certain number of previous filter response samples can be used as weight estimates without violating the accuracy requirements. Inclusion of $\eta_j(\mathbf{w})$ in (20) increases robustness of the filtering approach to anomalous data.

Table 6. Optimal variable-bandwidth filter settings for different conveyor belt speeds.

speed [m/s]	0.5	0.7	0.9	1.1	1.3
f_0^* [Hz]	66.5	49.0	35.5	39.0	32.5
f_∞^* [Hz]	0.1	0.1	0.1	0.1	0.1
α^*	5.35	4.65	3.97	3.90	3.46
k^*	3	3	3	3	3

The results of grid optimization, performed on the training data set, are summarized in Tab. 6. The results of final evaluation of the filter-based approach, obtained using the evaluation data set (i.e., the one that was not used for optimization purposes), are presented in Tab. 7. Note that the performance of the variable-bandwidth filter meets the accuracy specifications under all operating conditions. Fig. 5 shows a typical response of the optimized variable-bandwidth filter and the corresponding changes of the "cutoff frequency" $f_c(t)$.

Table 7. Experimental results obtained for the variable-bandwidth filtration approach.

speed		0.5	0.7	0.9	1.1	1.3
m_1	μ_e	-0.08	-0.10	-0.21	-0.02	-0.24
	σ_e	0.08	0.07	0.08	0.11	0.09
m_2	μ_e	-0.09	-0.03	-0.07	0.10	-0.26
	σ_e	0.15	0.13	0.12	0.14	0.14
m_3	μ_e	0.02	0.01	-0.05	0.31	-0.34
	σ_e	0.12	0.11	0.10	0.11	0.17
m_4	μ_e	0.04	0.11	-0.08	0.36	-0.41
	σ_e	0.12	0.15	0.17	0.12	0.22

5. CONCLUSION

In this case-oriented study two approaches to dynamic weighing, based on the system identification approach and on the variable-bandwidth filtering approach, were worked out and compared using experimental data produced by a conveyor belt type checkweigher. It was shown that when appropriately configured and tuned both approaches yield comparable, fully satisfactory results for all test loads and all conveyor belt speeds. The variable-bandwidth filtering approach is computationally less demanding but requires off-line optimization of filter parameters prior to weighing. The identification-based approach is computationally more involved but the resulting weighing algorithm operates in a fully adaptive way and hence is more robust.

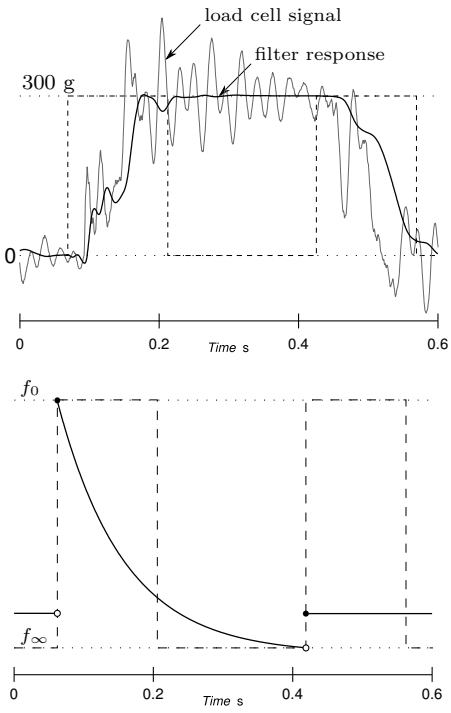

Fig. 5. Typical response of the optimized variable-bandwidth filter (upper figure) and the corresponding changes of the "cutoff frequency" $f_c(t)$ (lower figure).

REFERENCES

International recommendation OIML R 51-1 (2006). *Automatic checkweighing instruments. Part 1: Metrological and technical requirements - Test.*

McGuinness, M., Jenkins, D. & Senaratne, G. (2005). Modelling the physics of high-speed weighing. *Tech. Rep., Mathematics in Industry Information Service.*

Niedźwiecki, M. & Wasilewski, A. (1996). Application of adaptive filtering to dynamic weighing of vehicles. *Control Eng. Practice*, 4, 635–644.

Niedźwiecki, M. & Wasilewski, A. (1997). New algorithms for the dynamic weighing of trains. *Control Eng. Practice*, 5, 705–715.

Pietrzak, P. (2010). Dynamic mass measurement using a discrete time-variant filter. *Proc. IEEE IEEEI*, 151–155.

Piskorowski, J. (2008). Some aspects of dynamic reduction of transient duration in delay-equalized Chebyshev filters. *IEEE Trans. Instrum. Meas.*, 57, 1718–1724.

Piskorowski, J. & de Anda, M. (2009). A new class of continuous-time delay-compensated parameter-varying low-pass elliptic filters with improved dynamic behavior. *IEEE Trans. Circuits Syst.*, 56, 179–178.

Shu, W.-Q. (1993). Dynamic weighing under nonzero initial conditions. *IEEE Trans. Instrum. Meas.*, 42, 1347–1360.

Söderström, T. & Stoica, P. (1988). *System Identification.* Englewood Cliffs NJ: Prentice Hall.